Model test of a dual-spar floating wind farm in regular waves

Z. Jiang & G. Liang
Department of Engineering Sciences
University of Agder, N-4898 Grimstad, Norway

T. Lopez-Olocco & A. Medina-Manuel
CEHINAV, DACSON, ETSIN
Universidad Politécnica de Madrid, Spain

L.A. Saavedra-Ynocente
Laboratorio de Dinámica del Buque
Canal de Ensayos Hidrodinámicos el Pardo (INTA-CEHIPAR), 28048, Spain

A. Souto-Iglesias
CEHINAV, DACSON, ETSIN
Universidad Politécnica de Madrid, Spain

ABSTRACT: A floating wind farm with shared moorings has the potential to reduce capital expenditure but may face structural dynamics issues. We selected a prototype wind farm that consists of two spar floating wind turbines with shared moorings and carried out model tests with a scale factor of 1:47. Rigid-body motions of one spar and mooring line tensions were measured. In this paper, the test setup is described, and results from the decay and regular-wave tests are discussed. In regular waves, the spar motions in surge, heave, and pitch are dominated by wave frequencies and the extreme motion ranges are acceptable. Compared with the baseline, the clump weight affects the mean position of platform motion; it also reduces the dynamic tension of the shared line but causes higher mean and maximum tension in the single lines. This paper contributes to an improved understanding of complex floating systems in offshore environments.

1 INTRODUCTION

It has been more than a decade since the world's first megawatt-scale floating wind turbine (FWT), Hywind Demo, was commissioned in 2008. Today, although the technology readiness levels of several FWT concepts are high, many technical and economic challenges still exist for development of floating offshore wind farms (FOWFs); see (Jiang 2021). For example, to reduce the capital investment costs, solutions like shared anchors and concrete platforms are adopted in the Hywind Tampen farm which consists of eleven 8-MW spar FWTs.

Shared mooring stands as an alternative mooring solution with the potential of reducing the total number of mooring lines and anchors in an FOWF. Previously, pilot-scale FOWFs with shared moorings have been studied by several researchers, e.g., (Connolly & Hall 2019), (Liang et al. 2021). The foci of these references are on design and dynamics of the shared mooring systems and numerical methods are applied. To the authors' knowledge, no experimental work has been carried out to address FOWFs with shared mooring. For such a multibody structural system, hydrodynamic model tests are useful means and provide additional insights into the physical behavior of the system. To address this need, this paper documents interesting outcomes of a test campaign carried out at CEHIPAR in June 2022.

2 THE FLOATING WIND FARM WITH SHARED MOORING

The FOWF is a pilot-scale wind farm that consists of two spar FWTs. Each FWT has a draught of 120 m as specified for OC3-Hywind (Jonkman 2010). The two FWTs are placed along the x_g-axis with an initial turbine spacing of 750 m, approximately six times the rotor diameter. Two shared mooring configurations, 'baseline' and 'clump' are tested for the FOWF. As

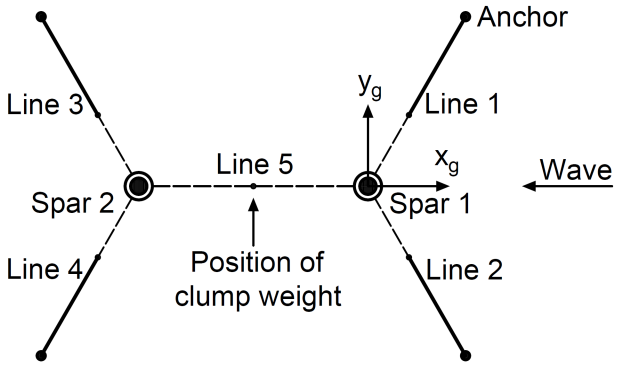

Figure 1: Schematic of a dual spar floating wind farm.

Table 1: Mooring properties of the selected single line design.

Parameter	Wire segment	Chain segment
Material	Sheathed steel wire	R3 Studless chain
Length [m]	250	415
Diameter [mm]	95	140
Sheath thickness [mm]	10	-
Mass per unit length [kg/m]	47.39	392.00
Submerged weight [N/m]	360.42	3535.94
Extensional stiffness [N]	8.47E+08	1.53E+09
Minimum breaking strength [N]	9.34E+06	1.43E+07

shown in Figure 1, each FWT is moored to the seabed by two single lines. For the baseline configuration, the two FWTs are connected together through a shared line (Line 5). For the clump configuration, a clump weight is added to the shared line; see Figure 1. The projected angle between any two adjacent mooring lines is 120 deg in the xy-plan.

For large-scale FOWFs with shared moorings, different mooring configurations can be adopted, and the present model can be regarded as the baseline. The baseline configuration was designed and studied previously (Liang et al. 2021, Liang et al. 2022). To accommodate the water depth of the ocean basin, a full-scale water depth of 235 m is considered. Therefore, the single lines of a spar FWT of OC3 Hywind were redesigned for the updated water depth. Details of the single line design can be found in (Lopez-Olocco et al. 2022). Mooring properties of the selected single line design are presented in Table 1. The unstretched length of the shared line is 739.6 m. The shared line is made of steel wire rope and its material properties is kept the same as the wire segment of the single lines.

3 MODEL TEST

3.1 *General*

Inertial and gravitational forces are important when it comes to testing of a floating structure in experimental environments. Therefore, the Froude similarity laws are chosen to scale down the mass and geometry of the OC3-Hywind spar platform (Jonkman 2010). Considering the depth limitation of the wave basin, a scale factor λ of 47 is selected. All structural elements of the dual-spar FOWF, including the spars and the mooring lines are scaled down based on this scale factor. Table 2 lists the the relation between the full- and model-scale physical parameters where the subscript p denotes 'full scale' and the subscript m denotes 'model scale'. Two configurations are considered, i.e., the first one with a pure shared line and the second one with a clump weight attached to the middle of the shared line.

Table 2: Conversion of physical variables according to the Froude similarity laws.

Parameter	Symbol	Scale factor
Length	L_p/L_m	λ
Linear velocity	v_p/v_m	$\lambda^{1/2}$
Linear acceleration	a_p/a_m	1
Angle	θ_p/θ_m	1
Angular velocity	ϕ_p/ϕ_m	$\lambda^{-1/2}$
Period	T_p/T_m	$\lambda^{1/2}$
Density	ρ_p/ρ_m	β
Displacement	$\triangle_p/\triangle_m$	$\beta\lambda^3$

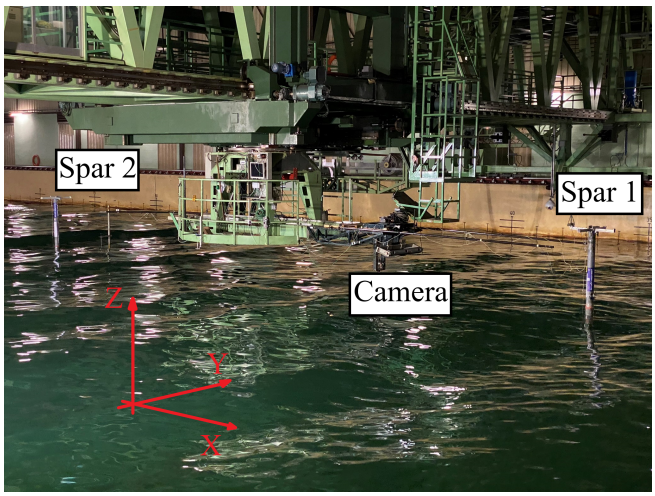

Figure 2: Image of the two FWT models during model tests; waves propagate from the right to the left.

Table 3: Mass and geometrical properties of the FWT.

Parameter	Full-scale	Model-scale
Mass [kg]	8.2372E+06	77.721
I_{xx} $[kgm^2]$	1.93E+10	84.39
I_{yy} $[kgm^2]$	1.93E+10	84.38
I_{zz} $[kgm^2]$	1.916E+8	0.69
CoG [m]	-78	-1.649
D_1 [m]	9.5	0.140
D_2 [m]	6.5	0.200
Draught [m]	-120	-2.54

Table 4: List of wave conditions of the regular wave tests.

Parameter	Full-scale		Model-scale	
	H [m]	T [s]	H [m]	T [s]
Operational	2.25	9.60	0.053	1.40
Extreme	10.0	16.0	0.213	2.33

3.2 *Model test set-up and instrumentation*

The full- and model-scale properties of the spar models are listed in Table 3. Here, CoG stands for center of gravity with the origin of the coordinate system at the mean water level. D_1 and D_2 refers to the lower and upper diameter of the spar, respectively. The mass distribution of the model represents that of OC3 Hywind, but rotor blades and wind loads were not explicitly addressed in the model tests. A thermoplastic material, polyvinyl chloride (PVC), was used as the main construction material. Lead panels were used as ballast and put inside each spar floater model. Additionally, to achieve the desired mass properties of the model, an aluminum structure with distributed weights was mounted on top of each PVC main structure.

Prior to the test, calibrated springs were attached to the anchor of the single lines to reproduce equivalent stiffness of the single lines and the shared line. Special care was taken to place the anchors at the exact locations as shown in the layout (Figure 1). In the second configuration, a cylindrical clumped weight was placed at the middle of the shared line. The submerged weight of the clump was 15 tonnes on full scale. Details of the model scaling and mooring system properties can be found in (Liang et al. 2022) and (Lopez-Olocco et al. 2022).

During the tests, the following measurements were obtained: six degree-of-freedom (DOF) motions of Spar 1; wave elevation at two different locations, i.e., one next to Spar 2 and the other at midway between the two spars; mooring tensions at two fairleads of the shared line and at three fairleads of the single lines of Spar 1.

All the instrumentation was calibrated before the formal tests to ensure the quality and reliability of the acquired data. For the motions a camera based optical tracking system was used. The water surface elevation was measured by means of a capacitance and an ultrasonic wave probe. Finally, the fairlead tension was obtained with the use of four one-component HBM load cells with an strain gauge full bridge. More details regarding the instrumentation and its uncertainties can be found in (Lopez-Olocco et al. 2022).

3.3 *Test matrix*

The test matrix of the load cases selected from the experimental campaign is detailed in Table 4. Two regular-wave conditions were tested for each mooring configuration. The operational condition represents mild sea states and the extreme condition represents survival conditions. No additional environmental load, e.g., wind or current, was considered. In addition, decay tests for the 6 DOF in Spar 1 were performed to obtain the natural periods and damping level of the FOWF in different DOFs.

Table 5: Natural periods of Spar 1 identified from decay tests [s].

DOF	Baseline	Clump
Surge	142.88	134.15
Sway	83.89	79.96
Heave	30.50	30.55
Roll	31.56	31.40
Pitch	31.62	31.45
Yaw	23.93	22.38

4 RESULTS

In this section, we present results from the model tests in the order of decay test, and regular wave tests in both operational and extreme conditions. A focus is placed on the time series.

4.1 *Natural periods of the dual-spar system*

Natural periods, mode shapes, and damping of a moored marine structure are important properties that characterize the structural dynamics. For an interconnected dual-spar FOWF with a mooring design for a deepwater site (water depth=320 m), Liang et al. (2021) linearized the system stiffness and identified 12 natural periods and mode shapes. Here, the natural periods identified from the free decay excitations of Spar 1 are listed in Table 5. Due to test limitation, it was not possible to excite or measure both spars, and only six modes are obtained. The identified surge mode has a natural period of more than 130 seconds; the other surge mode exists with a much lower natural period. Compared with the baseline configuration, the shared line configuration with the clump weight causes an approximately 6.1% reduction in the surge natural period and 4.7% reduction in the sway natural period, whereas the influence on the other DOFs is relatively small. This observation is expected, as the clumped weight (15 tonnes on full scale) increases the mooring stiffness.

4.2 *Regular wave test*

In this section, the time histories of the model tests are presented on full scale and discussed. Among the various response variables, the platform motion response in surge, heave and pitch DOFs and the mooring tension responses of both the single and shared lines at

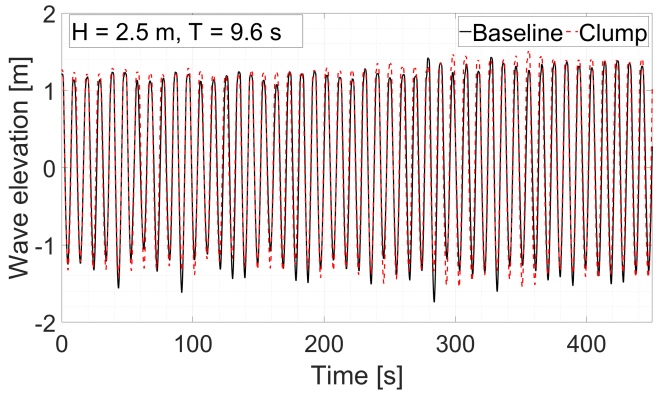

Figure 3: Comparison of the wave elevation, operational wave condition.

fairleads are selected. The platform motion response of Spar 1 is presented with respect to its static equilibrium positions in two configurations, respectively.

4.2.1 *Operational wave condition*

The absolute elevations of the generated regular waves were obtained from a measurement point located next to Spar 2 and are shown in Figure 3. The presented sea state is called operational condition because it has a relatively high probability of occurrence and the FWTs are expected to be in operation. Although the wave elevations are regular, small fluctuations are observed for the peak wave amplitudes for both configurations.

Figure 4a presents the platform surge motion of Spar 1. As shown, the surge motion of the spar is dominated by wave frequency-induced first-order motions. In addition, slowly-varying motion of the spar can be clearly observed in the time history of both cases. This slowly-varying period corresponds to the longer surge mode of the dual-spar system. Compared to the baseline configuration, the clump configuration reduces the motion range and results in lower second-order responses due to the increase in the mooring stiffness in surge.

Figure 4b and Figure 4c shows the platform heave motion and pitch motion, respectively. Although both the heave and pitch DOFs are dominated by wave-frequency responses, the heave motion is more affected by the clump weight than the pitch motion. As shown in Figure 4b, the response maxima of the platform heave under the clump case is slightly higher than those under the baseline case. This observation is because the presence of the clump weight draws the two spar FWTs closer to each other and reduces the vertical mooring stiffness provided by the two single lines. Compared to the shared line, the single lines play a more important role in providing restoring stiffness in the heave DOF in addition to the hydrostatic stiffness. As shown in Figure 4c, the difference between the baseline case and the clump case in the mean and maximum values of the platform-pitch motion is limited. This observation is expected as the present shared mooring system, with or without additional clump weight on the shared line, provide limited pitch restoring stiffness for the spar platform motion in waves. The restoring moment created by the buoyancy and gravity forces govern.

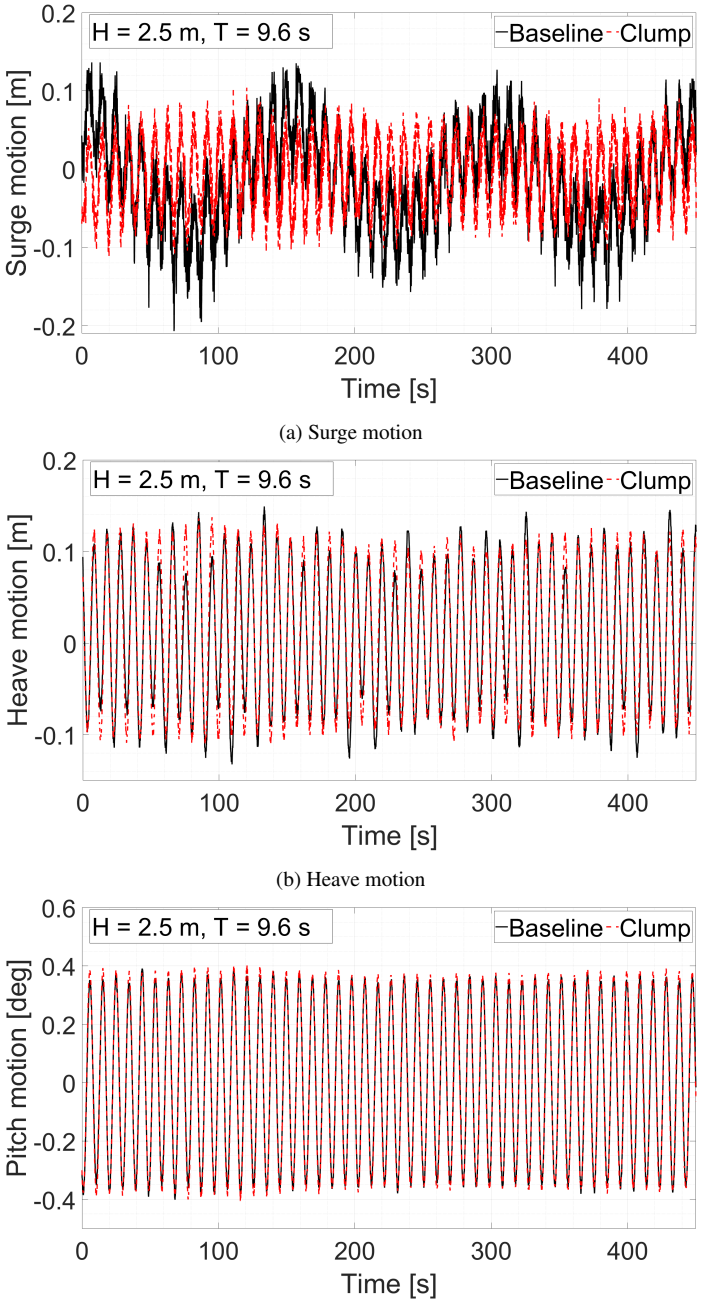

(a) Surge motion

(b) Heave motion

(c) Pitch motion

Figure 4: Comparison of the platform motion, Spar 1, operational wave condition.

Time histories of the top tension of the mooring Line 1 and the shared line (at the attachment point of Spar 1) is presented in Figure 5a and Figure 5b, respectively. As the vertical positions of the fairleads lie between the buoyancy and gravity centers of Spar 1, the fairlead motion is strongly affected by the rigid body motions of the spar buoy in surge, heave, and pitch DOFs. As these motions are dominated by the wave period of the regular waves, the oscillation periods of Tension T_1 and Tension T_{5f1} are also close to this period. In addition, two interesting observations can be found from the figures by comparing the ten-

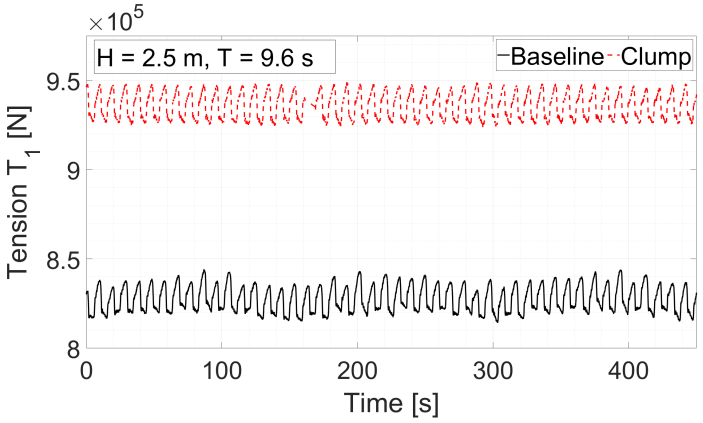

(a) T_1

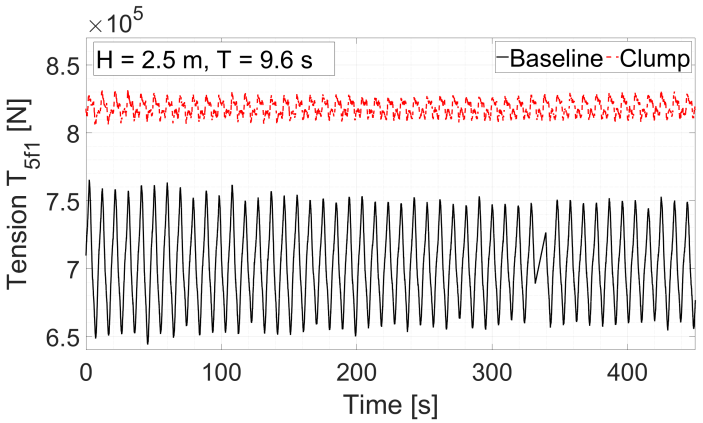

(b) T_{5f1}

Figure 5: Comparison of the mooring tension, operational wave condition.

sion responses of the baseline and clump weight configurations. First, the mean tension in both the single line and the shared line increases after the clump weight is used. The mean tension is influenced by the pretension of the moorings in the static position and the mean drift forces of the waves. As the clump weight is placed in the middle of the shared line, this additional weight has a more appreciable influence on the shared line than on the single lines. The pretension and the mean tension are increased by the submerged weight of the clump (15 tonnes). Second, for this operational sea state, the dynamic tension of the shared line is significantly reduced ($> 70\%$) after the clump weight is used, whereas dynamic tension of the single line is on a similar level. Although the effect of the clump will depend on the weight, number, and location, this observation indicates the potential of clump in reducing the dynamic tension and hence fatigue damages of the shared line.

4.2.2 *Extreme wave condition*

In the following, time histories from the extreme sea state (H=10 m, T=16 s) are analyzed. As shown in Figure 6, although the measured wave signal is quite regular and has better quality than that of the operational sea state, the measured wave height slightly exceeds 10 m on full scale. As these waves reflect the actual measurements and are not the calibrated waves,

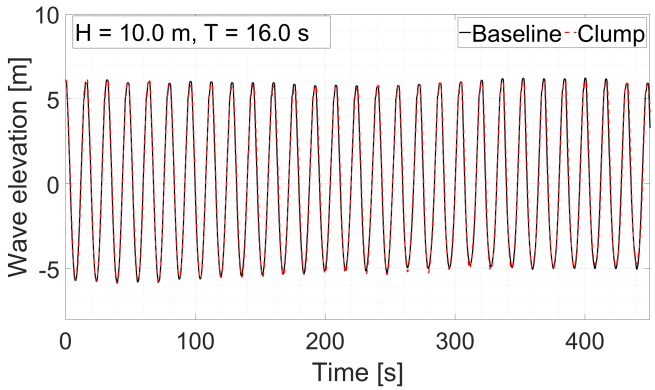

Figure 6: Comparison of the wave elevation, extreme wave condition.

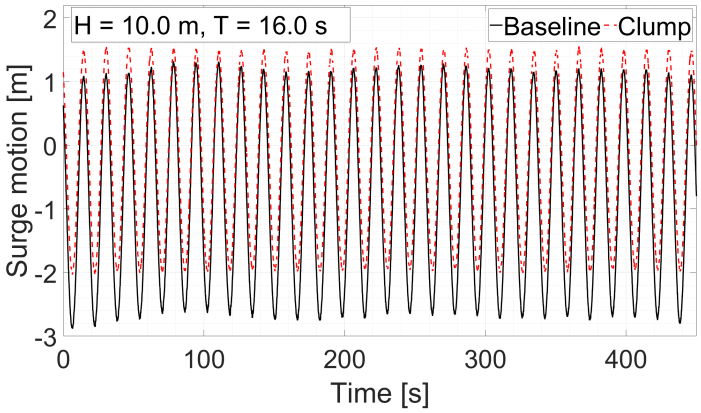

(a) Surge motion

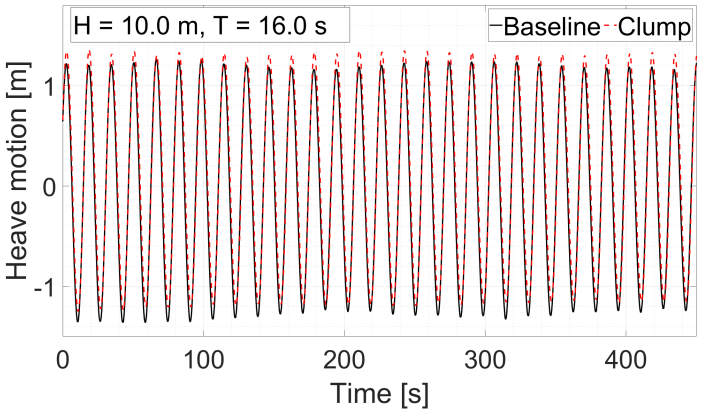

(b) Heave motion

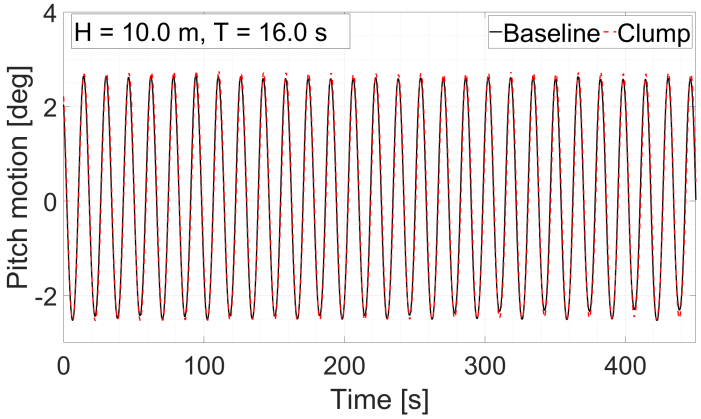

(c) Pitch motion

Figure 7: Comparison of the platform motion, Spar 1, extreme wave condition.

the small difference ($<5\%$) of the wave amplitude

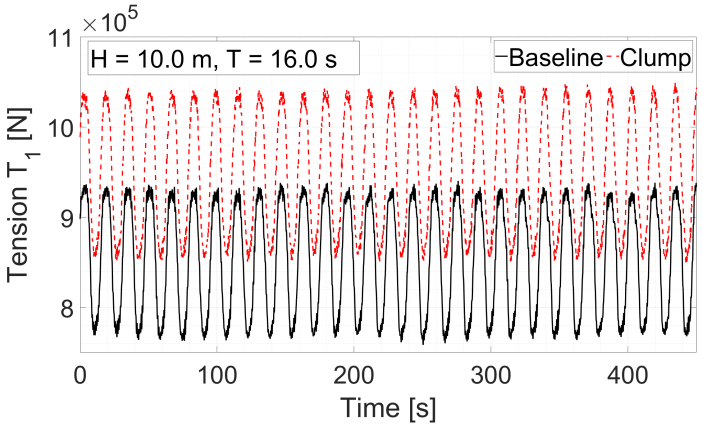

(a) T_1

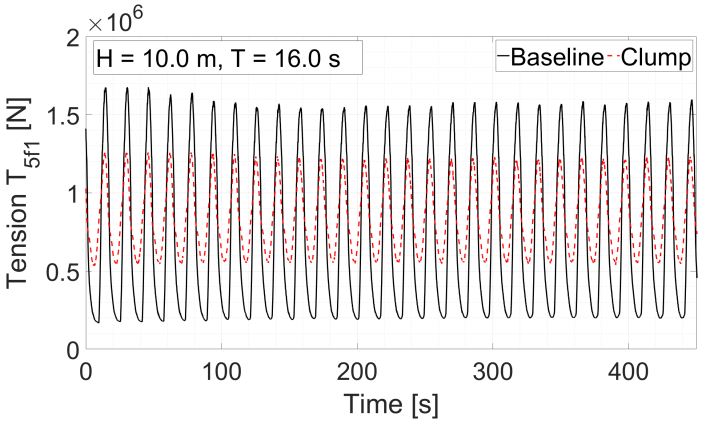

(b) T_{5f1}

Figure 8: Comparison of the mooring tension, operational wave condition.

from the expected value can be deemed acceptable.

Figure 7a presents the platform surge motion of Spar 1 under the extreme sea state. As shown, the response is still dominated by the wave frequency. Although a slowly varying component is also present in the surge response, the effect is not strong. This can be explained by the fact that the transfer function of the mean drift force of a spar buoy reduces quickly as the period increases according to the potential flow-based hydrodynamic analysis. Compared with the baseline configuration, the clump weight also results in a change in the mean surge position of Spar 1.

Figure 7b and Figure 7c show the heave and pitch motions of Spar 1. From the figures, it is observed that the magnitudes of the heave and pitch motions are quite large because of the small damping for the system. For example, with the baseline configuration, Spar 1 has a damping ratio of approximately 1.9% for the heave DOF and approximately 1.3% for the pitch DOF. This damping level is similar to that of a single spar with three mooring lines; see (Lopez-Olocco et al. 2022). For design of FWT systems, common design guidelines, e.g., DNV-ST-0119 (DNV 2018), does not specify any criteria for the maximum allowable platform motions. In literature, a maximum platform pitch of 10 deg was considered by Pereyra et al. (2018) and a maximum platform heave of 7 m was mentioned by Allen et al. (2020). The present motion range of the spar with both mooring configurations is acceptable considering these criteria. The influence of the clump weight on the motion response of heave and pitch is similar to the one under the operational sea state. The chosen clump weight increases the mean and maximum heave motion and the effect on the platform-pitch motion is rather limited.

Extreme offshore environmental conditions are important in the design load cases for mooring systems (DNV 2015). For the mooring system of the proposed baseline FOWF, component properties of the single mooring lines were chosen following the design procedure for a single spar FWT with three mooring lines (Liang et al. 2021). As shown in Figure 8a, compared with the baseline configuration, the clump weight configuration causes an increase in the mean and peak tension of mooring Line 1 (T_1) by approximately 100 kN in the extreme wave condition. This increase is similar to that in the operational wave condition and is primarily due to the changed mean position of the spars due to the increased shared line weight. Still, the increased peak tension indicates that a further design check is needed for the single lines in the extreme wave conditions. Interestingly, for this extreme condition, the shared line tension becomes a critical consideration in the mooring system design, as the peak load of the shared line (Tension T_{5f1}) exceeds that of the mooring Line 1 (Tension T_1) by more than 50%. Application of the clump weight results in a substantial reduction in the dynamic tension and the peak loads of the shared line. It is also expected that the clump weight will alleviate the snap load events experienced by the shared mooring system in irregular wave conditions (Liang et al. 2022). Note that the tension of mooring Line 2 (tension T_2) of Spar 1 is also measured. As the present mooring system is symmetrical with regard to the wave heading (see Figure 1), the time history of tension T_2 is similar to that of T_1 and is not shown here.

5 CONCLUDING REMARKS

In this paper, the regular wave model test outcomes are presented of a dual spar floating wind farm with two shared mooring configurations. The baseline mooring system has two-segment single lines for each spar platform and one shared line (made of steel wire). The other mooring configuration has the same single lines for the spars, but the shared line has a clump weight attached to its midspan. By analyzing the platform motion responses of Spar 1 and mooring tension at the fairleads, the main conclusions are as follows:

- In both the operational wave condition (H=2.5 m, T=9.6 s) and the extreme wave condition (H=10 m, T=16 s), the platform motion responses of the spar with shared mooring in

surge, heave, and pitch are dominated by the wave-frequency responses, and second-order responses are also observed in the surge motion. The maximum platform pitch and heave motions in the extreme wave condition are well below previously documented allowable limits for floating offshore wind turbines.

- For the platform surge motion, the addition of a submerged clump weight of 15 tonnes (on full scale) to the shared line decreases the maximum value and second-order response under the operational wave condition, and slightly increases the mean and maximum values under the extreme wave condition. The influence on the platform heave motion is secondary, and there is limited influence on the platform pitch motion. These effects are primarily due to changes in the mooring stiffness.

- In the extreme wave condition, the shared line has higher peak values in the tension than the single mooring line.

- Compared with the baseline mooring configuration, the clump weight configuration shows substantially higher mooring tension (both mean and maximum) in the single lines. This indicates additional design check for the design of single mooring lines.

- The considered clump weight effectively reduces the dynamic tension of the shared line and can potentially alleviate the fatigue damage and snap load events. A study varying the position, number and weights of the clumps can be considered in the future.

REFERENCES

Allen, C., Viscelli, A., Dagher, H., Goupee, A., Gaertner, E., Abbas, N., Hall, M., & Barter, G. 2020. Definition of the UMaine VolturnUS-S reference platform developed for the IEA Wind 15-megawatt offshore reference wind turbine. Technical report, National Renewable Energy Laboratory, Golden, CO (United States).

Connolly, P. & Hall, M. 2019. Comparison of pilot-scale floating offshore wind farms with shared moorings. *Ocean Engineering 171*, 172–180.

DNV 2015. Offshore standard DNV-OS-E301, Position mooring. Høvik, Norway.

DNV 2018. Standard DNV-ST-0119, Floating wind turbine structures. Høvik, Norway.

Jiang, Z. 2021. Installation of offshore wind turbines: A technical review. *Renewable and Sustainable Energy Reviews 139*, 110576.

Jonkman, J. 2010. Definition of the Floating System for Phase IV of OC3. Technical Report NREL/TP-500-47535, National Renewable Energy Lab.(NREL), Golden, CO (United States).

Liang, G., Jiang, Z., & Merz, K. 2021. Mooring analysis of a dual-spar floating wind farm with a shared line. *Journal of Offshore Mechanics and Arctic Engineering 143*(6), 062003.

Liang, G., Jiang, Z., & Merz, K. 2022. Dynamic analysis of a dual-spar floating offshore wind farm with shared moorings in extreme environmental conditions. Submitted for publication.

Liang, G., Lopez-Olocco, T., Medina-Manuel, A., Saavedra-Ynocente, L., Jiang, Z., & Souto-Iglesias, A. 2022. Experimental investigation of two shared mooring configurations for a dual-spar floating offshore wind farm in irregular waves. Submitted for publication.

Lopez-Olocco, T., Liang, G., Medina-Manuel, A., Saavedra-Ynocente, L., Souto-Iglesias, A., & Jiang, Z. 2022. Experimental study of a shared-mooring and a catenary mooring system for spar floating wind turbines under regular and irregular waves. Submitted for publication.

Pereyra, B. T., Jiang, Z., Gao, Z., Andersen, M. T., & Stiesdal, H. 2018. Parametric study of a counter weight suspension system for the TetraSpar floating wind turbine. In *International Conference on Offshore Mechanics and Arctic Engineering*, Volume 51975, pp. V001T01A003. American Society of Mechanical Engineers.